Eur. Phys. J. E **6**, 79–89 (2001)

THE EUROPEAN PHYSICAL JOURNAL E

EDP Sciences

A minimal model for vorticity and gradient banding in complex fluids

J.L. Goveas[1,a] and P.D. Olmsted[2,b]

[1] Department of Chemical Engineering, MS 362 Rice University, 6100 Main Street, Houston, TX 77005, USA
[2] Polymer IRC and Department of Physics & Astronomy, University of Leeds, Leeds LS2 9LT, UK

Received 1 April 2001 and Received in final form 16 June 2001

Abstract. A general phenomenological reaction-diffusion model for flow-induced phase transitions in complex fluids is presented. The model consists of an equation of motion for a nonconserved composition variable, coupled to a Newtonian stress relation for the reactant and product species. Multivalued reaction terms allow for different homogeneous phases to coexist with each other, resulting in banded composition and shear rate profiles. The one-dimensional equation of motion is evolved from a random initial state to its final steady state. We find that the system chooses banded states over homogeneous states, depending on the shape of the stress constitutive curve and the magnitude of the diffusion coefficient. Banding in the flow gradient direction under shear rate control is observed for shear-thinning transitions, while banding in the vorticity direction under stress control is observed for shear-thickening transitions.

PACS. 47.20.Ft Instability of shear flows – 47.20.Hw Fluid dynamics: Morphological instability; phase changes – 05.45.-a Nonlinear dynamics and nonlinear dynamic systems – 05.70.Ln Nonequilibrium and irreversible thermodynamics

1 Introduction

There is a significant body of experimental evidence documenting the existence of sharp, stable interfaces separating two or more phases or "bands", in shear flow in complex fluids. This phenomenon has been reported in various types of surfactant solutions [1,2], polymers [3], liquid crystals [4] and colloidal suspensions [5]. There appears to be a compelling generality between these "phase transitions" in different complex fluids:

i) The onset of banding or phase separation manifests itself as a discontinuity in the "flow curve" of the system. The flow curve is the unique relationship between the measured shear stress and the applied shear rate (or vice versa) at steady state. An experimental flow curve typically contains segments that correspond to homogeneous flow, as well as segments corresponding to inhomogeneous flow. The individual homogeneous bands that make up the inhomogeneous state each have their own homogeneous flow curve, which we shall refer to as a "constitutive curve". The inhomogeneous flow curve then represents the response of the system, averaged over different spatial regions that occupy different homogeneous flow branches, in proportions to maintain the externally controlled shear stress or shear rate. (Henceforth we will use the terms stress and shear stress interchangeably, unless otherwise specified.)
ii) The transition only occurs above a unique and reproducible critical stress or shear rate.
iii) The flow curve can be qualitatively different depending on whether the average stress or the average shear rate in the system is held fixed. (In a typical rheological experiment this is achieved by controlling the torque or angular velocity, respectively.) For intermediate stresses or shear rates, the flow curve usually has multiple branches that are not equally accessible under both stress and shear rate control. For weak and strong flows, the flow curve is single-valued, and the same locus of points is traced out under stress or shear rate control.
iv) The flow-induced bands have different shear rates or shear stresses, and are generally also distinguished by some combination of different degrees of order and different microstructures.
v) The interfaces between the bands may be aligned in the direction of the flow gradient or the flow vorticity. Each banding orientation has its own rheological signature. In shear-thinning systems, for example, a stress plateau in the flow curve usually indicates gradient banding, while extrema in the stress (as a function of shear rate) usually indicate vorticity banding. One of us [6] has constructed possible flow curves based

[a] e-mail: jlgoveas@rice.edu
[b] e-mail: p.d.olmsted@leeds.ac.uk

on the banding orientation and the character of phase coexistence (shear thinning *vs.* shear thickening).

Gradient banding has been unambiguously observed in solutions of wormlike micelles. In strain-controlled experiments on shear-thinning solutions, a stress plateau coincides with shear banding in the gradient direction [7]. In shear-thickening solutions [1], a gel-like phase can be induced by flow. Under shear rate control the induced phase fills the system at steady state, resulting in a discontinuous stress jump in the flow curve. Under stress control phase coexistence between solution and gel is observed, the gel fraction being an increasing function of stress. In the corresponding flow curve the shear rate shows a minimum and maximum. In bcc cubic crystals of triblock copolymers [3], Eiser *et al.* observed two stress plateaus in the flow curve under controlled shear rate. X-ray diffraction shows that each plateau corresponds to different orientations (relative to the flow direction) of dense planes in the crystal.

Vorticity banding has been reported in dense colloidal suspensions [5] and surfactant solutions of multilamellar vesicles [2]. When the shear rate is held fixed, the flow curve shows a maximum and minimum in the stress. Under controlled stress, there is a jump up in shear rate upon increasing stress, and a jump down in shear rate upon decreasing stress. The same qualitative curves have also been observed in surfactant hexagonal phases [8], although in that case vorticity banding has not yet been explicitly verified. Such behavior is analogous to that of the shear-thickening wormlike micelles, if the roles of stress and shear rate are interchanged.

In steady state there can be no acceleration, so the total stress must be divergence free. In planar shear flow, this implies that the shear rate in the vorticity direction and the shear stress in the gradient direction are uniform. Vorticity banding thus corresponds to a scenario where bands share a common shear rate but can have different shear stresses (see Fig. 1). Similarly, when bands lie in the gradient direction the stress is uniform across the bands and the shear rate can vary. Most experiments where banding has been observed have been carried out in the curved geometries of cone-and-plate or Couette rheometers. The gaps in these rheometers are usually very thin, and in this limit the flow is approximately a planar shear flow. (We also note that we consider flows in the Stokes' flow limit.)

The microscopic mechanisms causing the transitions in all these complex fluids are likely to be highly system specific, and govern the critical shear rate or shear stress, the structure of the flow-induced phases, and the detailed shape of the flow curves. At a macroscopic level, however, there appears to be a high degree of universality between systems. As we have discussed, different complex fluids can produce qualitatively similar flow curves. By simply analysing the shape of these flow curves, we have extracted information about the banding orientation of the transition [6], as well as the stability of the system [9].

The obvious analog to this way of thinking is the well-known Landau-Ginzburg theory of equilibrium phase transitions. A free-energy functional consisting of a double-well local free energy and a square gradient term reproduces all the phenomenology of a phase transition in the region of the critical temperature, for many different systems. However, a microscopic theory is required to calculate the Landau coefficients. In this work, we use a multivalued reaction diffusion scheme to construct a general phenomenological theory to describe phase transitions in flow; in the spirit of Landau-Ginzburg theory, such a model could in principle be derived from microscopic theories.

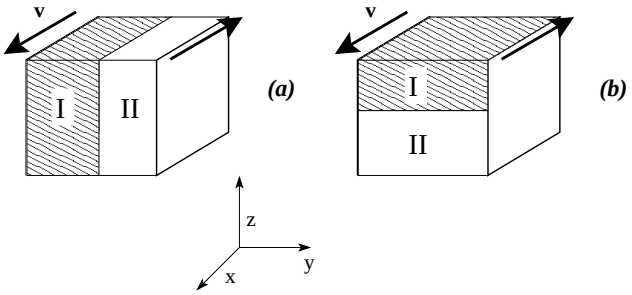

Fig. 1. a) Gradient banding: flow-induced phases lie in the direction of the velocity gradient (arrow shows flow direction). The bands share the same shear stress, but can have different shear rates. b) Vorticity banding: bands lie in the flow vorticity direction. Here, the shear rate is uniform across the bands, but the shear stress can vary from one band to the other.

The most difficult step in devising such a nonequilibrium theory is determining the important variables. Typically there are three significant quantities: i) a species concentration, which is a conserved scalar, ii) the momentum density, which is a conserved vector and iii) the stress, which is a nonconserved tensor. The momentum density is described by the Navier-Stokes equation, and its current is the stress. In addition, nonconserved "microstructural" order parameters exist that contribute to the stress. These may be scalars such as chain length in wormlike micelle solutions, or tensors such as molecule orientation. Since all of these variables have different relative relaxation times, one must distinguish between slow variables, which require their own equations of motion, and fast variables, which relax quickly to a steady-state value.

The choice of slow variables affects the structure of the equations of motion and the couplings between them, and therefore the dynamics of the system. In models of hydrodynamic instabilities, for example, the momentum is considered to be a slow variable. A phenomenological stress constitutive equation is often used: if the stress is taken to be a fast variable, this relation is simply an algebraic function of the rate of strain tensor, such as the Newtonian relation for simple fluids; if the stress is taken to be a slow variable, this relation takes the form of a differential equation, such as the Upper Convected/Oldroyd-B Maxwell model for polymer melts. The hallmark of complex fluid rheology, however, is the coupling between the velocity and/or the stress and the microstructure of the fluid. In microscopic theories, generally an equation of motion is not written for the total stress, but for another slow variable that makes an important contribution to it, such

as the director in nematic liquid crystals or the second moment of the configuration tensor in polymer melts.

Schmitt, Marques and Lequeux [10] have classified flow instabilities in complex fluids as "mechanical" or "spinodal" instabilities, using a model where concentration and momentum are the slow variables. If a perturbation to the shear rate first makes the system go unstable, the instability is mechanical, while it is spinodal if the concentration becomes unstable first. Note that "instability" as is used here refers to a linear instability. Any instability, linear or nonlinear (we return to this issue at the end of the paper), can lead to a macroscopically shear-banded state that resolves the instability.

Shear banding associated with momentum instabilities have been analyzed in detail at a high (macroscopic) level, using the phenomenological Johnson-Segalman model [11–13]. Here a nonconserved "polymer" stress tensor, playing the role of the slow variable, is included in the total stress, resulting in a multi-valued stress constitutive relation. This model produces gradient banding and a flow curve with a stress plateau, and is considered a reasonable mimic of shear-thinning wormlike micelles. Microscopically derived theories for wormlike micelles [14] and nematic liquid crystalline melts [15] yield a nonmonotonic relation similar to the Johnson-Segalman model, but with the benefit of a molecular interpretation.

An alternative caricature to these models has been developed in phenomenological theories for shear thickening. Originally, Ajdari [16] proposed an equation of motion for the position of an interface that separates high- and low-viscosity phases under shear. By coupling this equation with conservation laws and a Newtonian stress constitutive equation for the micellar solution, a nonmonotonic flow curve was produced. Goveas and Pine adopted this approach to describe shear-thickening wormlike micelles and were able to successfully reproduce much of the experimental phenomenology. The flow curve was then used to explain the differences in stress *vs.* shear rate control, based on a linear-stability analysis of the interfacial height equation. In this case, the momentum and micellar solution stress were taken to be fast variables, while an equation of motion was written for a scalar variable, which is the macroscopic manifestation of changes in the fluid microstructure.

However, the formulation of Goveas and Pine did not contain any mechanism for the formation of the shear-induced state, so that the *existence* of the new phase was simply postulated by the presence of an interface with its own dynamics. In this paper we present a generic phenomenological model that admits a flow-induced phase, and incorporates spatial gradients. The interface structure and its stability emerge naturally from the steady-state conditions of this model. The inclusion of spatial gradients (or interface stability) is a necessary condition to resolve the coexistence criteria of shear-induced phases [17].

The model consists of a reaction-diffusion equation of motion for the volume fraction of a reacting species, *i.e.* a scalar nonconserved order parameter representing microstructural change in a complex fluid. There are fast stress variables associated with the reactant and product species, which contribute additively to the total stress. We have continuously evolved the model from a homogeneous to a phase-separated state, and examined how thinning and thickening flow curves, as well as the size of the gradient terms, affect phase transitions, and in particular the banding orientation (vorticity *vs.* gradient banding). Most significantly, we are able to probe the nonlinear dynamic behavior of the system.

2 Minimal model

Our phenomenological theory consists of a general reaction-diffusion scheme. The reaction terms represent the creation and destruction of a variable under flow, and are analogous to the local free-energy terms in a Landau-Ginzburg theory. This variable may embody a species concentration, or a structural parameter such as aggregate size or molecule orientation. While this scheme is meant to be quite general and is a vehicle for capturing the general physics for many complex fluids, a reaction diffusion scheme has a literal basis for wormlike micelles and onion solutions. In the wormlike micelle case, such "reaction" terms correspond to the constant breaking and recombination of the "living" polymers; while in onion solutions, the reaction terms might correspond to the formation of onions. The steady-state onion size scales as the inverse square root of the shear rate [18] and is a reversible function of the shear rate; *i.e.* the size is independent of whether smaller onions are created by increasing the shear rate applied to larger onions, or larger onions are created by decreasing the shear rate applied to smaller onions. This indicates that onion combination and fracture processes compete to attain steady state, and these processes have different dependences on shear rate.

Consider a system that is one-phase at equilibrium, and consists solely of a species, A. Planar shear flow is then applied to this system: the coordinate system is shown in Figure 1, where x, y and z denote the flow, gradient and vorticity directions, respectively. We consider only variations in y and z in this work. Suppose that a new phase, B, can be induced by flow, such that at a given shear rate (or stress) a dynamic equilibrium between A and B is established. We write this schematically as

$$A \rightleftharpoons B\,. \tag{2.1}$$

Let us define an order parameter, $\phi_B \equiv \phi$, which corresponds to the volume fraction of the B-species (although allowing ϕ to correspond to a structural variable is also viable). The system is constrained to have constant density such that

$$\phi_A + \phi_B = 1\,. \tag{2.2}$$

Notice that ϕ_A and ϕ_B are nonconserved variables, although the total density is conserved. We write the following equation of motion for ϕ as

$$\frac{\partial \phi}{\partial t} = R(\phi, \dot\gamma) + D\nabla^2\phi\,, \tag{2.3}$$

where $R(\phi, \dot{\gamma})$ represents the forward and backward "reactions" that create and destroy the new phase, $\dot{\gamma}(y, z) = \mathrm{d}v_x/\mathrm{d}y$ is the local shear rate (where v_x is the component of the velocity in the flow direction), and D is an effective diffusion coefficient (taken to be a constant).

The dynamics modelled by equation (2.3) are equivalent to the relaxational dynamics of a nonconserved order parameter, ϕ, for an equilibrium phase transition. The right-hand side of equation (2.3) corresponds to $-\delta F/\delta\phi$, where $F(\phi) = \int \mathrm{d}x[f(\phi) + \frac{1}{2}D(\nabla\phi)^2]$ is the free-energy functional (within a square-gradient theory). $R(\phi, \dot{\gamma})$ is analogous to the derivative $-\partial f(\phi)/\partial\phi$. In the same way that a double well potential in the free energy signals the possibility of equilibrium phase coexistence, a multivalued reaction term can allow for flow-induced banding.

The diffusion terms in equation (2.3) are the analog of the nonlocal terms in the free energy and provide gradients that can support inhomogeneities and describe interfaces between states. The diffusion coefficient is thus a measure of the interfacial tension in the system, and its magnitude is proportional to the square of the interfacial width. However, unlike at equilibrium, where a global minimization principle applies, the diffusion terms are necessary for determining the conditions for phase coexistence in flow [17] (see next section).

3 Constitutive curves

To compute flow curves for the system, stress constitutive equations for the different components must also be specified. The simplest possible scheme involves additive Newtonian relations for each species

$$\sigma = \sigma_A + \sigma_B\,, \qquad \sigma_\alpha = \eta_\alpha \phi_\alpha \dot{\gamma}\,, \tag{3.1}$$

where σ is the total shear stress, and σ_α and η_α are the shear stress and viscosity, respectively, of species $\alpha = A, B$. Stress and composition are thus effectively coupled in the system. Applying the density constraint, equation (2.2), gives an expression for the constitutive curve of the system,

$$\sigma = [\phi(c-1)+1]\dot{\gamma}\,, \tag{3.2}$$

where $\phi = \phi(\dot{\gamma})$ is the solution to equation (3.3), $c = \eta_B/\eta_A$ is the ratio of the viscosities of the two components, and we have set $\eta_A = 1$ for simplicity.

The *homogeneous* steady-state solutions to equation (2.3), where $\nabla^2\phi = 0$, are given by

$$R(\phi, \dot{\gamma}) = 0\,. \tag{3.3}$$

A multivalued $R(\phi, \dot{\gamma})$ thus leads to more than one homogeneous steady state for equation (2.3.) This in turn produces a constitutive curve with multiple branches, via equation (3.2). In this paper, we choose the following form for $R(\phi, \dot{\gamma})$:

$$R(\phi, \dot{\gamma}) = |\dot{\gamma}|\phi_A\phi_B^2 - k\phi_B\,, \tag{3.4}$$

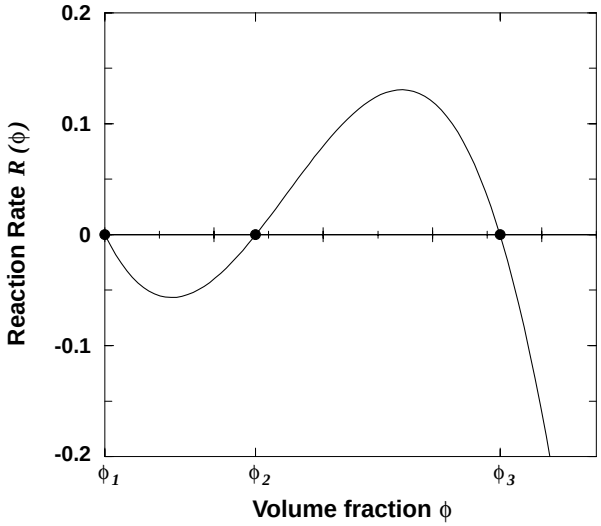

Fig. 2. Multivalued reaction scheme (see Eq. (2.3)) which produces three possible roots, ϕ_1, ϕ_2 and ϕ_3, corresponding to stable, unstable and stable homogeneous states, respectively, for a fixed value of the shear rate.

which yields the curve shown in Figure 2, for an imposed $\dot{\gamma}$. In equation (3.4) k represents a rate constant for a backward reaction, which has dimensions of inverse time and is henceforth set to unity. This scheme might be given the physical interpretation of a reaction pathway where both A and B molecules participate to form B molecules, but B molecules can disintegrate on their own to form A molecules. We stress, however, that our model is purely phenomenological and does not as such apply to any specific system. Certainly, other multi-valued functional forms could be chosen for $R(\phi, \dot{\gamma})$, which would also result in a multi-valued constitutive curve.

The forward reaction term in equation (3.4) has a linear shear rate dependence, so we must take its absolute value from symmetry considerations. In microscopic theories for flow-induced reactions in wormlike micelles [19] and polymers [20], such an *effective* reaction rate also has a linear or nonanalytic form, resulting from the projection of tensorial degrees of freedom onto a scalar order parameter. Reaction terms with nonlinear and nonanalytic flow rate dependences are, of course, also conceivable.

For a given local shear rate, the reaction scheme of equations (2.2, 3.3, 3.4) yields the following homogeneous steady states:

$$\phi_1 = 0\,, \tag{3.5a}$$

$$\phi_2 = \frac{1}{2} - \frac{1}{2}\sqrt{1 - \frac{4}{\dot{\gamma}}}\,, \tag{3.5b}$$

$$\phi_3 = \frac{1}{2} + \frac{1}{2}\sqrt{1 - \frac{4}{\dot{\gamma}}}\,. \tag{3.5c}$$

Performing a linear-stability analysis on equation (2.3), at fixed $\dot{\gamma}$, shows that ϕ_1 and ϕ_3 are stable fixed points for the system, while ϕ_2 is an unstable fixed point. This is

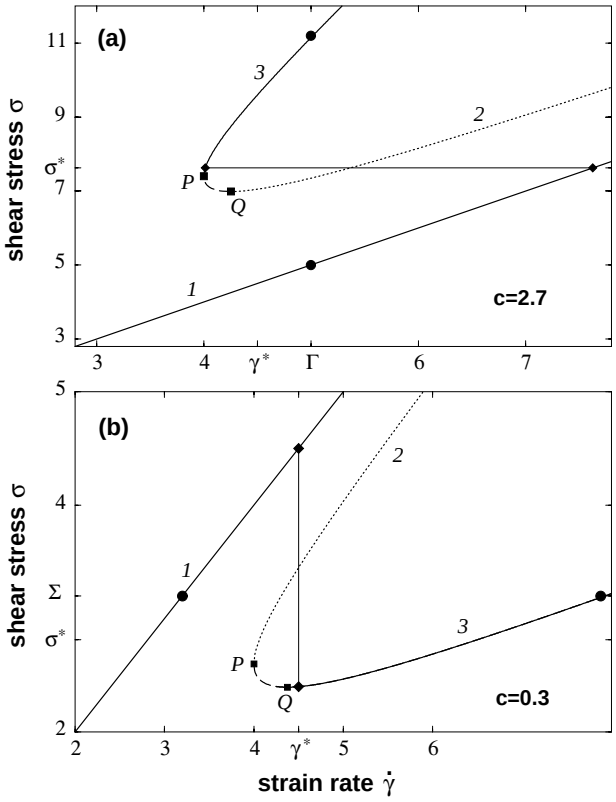

Fig. 3. Flow curves (from Eqs. (3.3, 3.2) and (3.4)) corresponding to the minimal model. At low shear rates, the flow curve is single-valued (branch 1). Above a certain shear rate (or stress), an additional unstable branch, 2, and a stable branch, 3, exist. These branches correspond to the homogeneous roots $\{\phi_1, \phi_2, \phi_3\}$ from equations (3.5) for imposed shear rate, and $\{\phi_1, \phi_2', \phi_3'\}$ from equations (3.8) for imposed stress. In the former case, branches 2 and 3 are separated by P, while they are separated by Q in the latter. Thus, the line segment between P and Q is stable under controlled shear rate, but unstable under controlled stress. (a) Shear-thickening flow curve for $c > 1$, illustrating the controlled shear rate case. At a fixed shear rate, Γ, the system can choose between homogeneous states on branches 1 and 3, or gradient band between these branches at stress σ^*. (b) Shear-thinning flow curve for $c < 1$, illustrating the controlled stress case. At fixed stress Σ, the system can vorticity-band at shear rate $\dot{\gamma}^*$ between 1 and 3, or choose between homogeneous states on these same branches.

evident from Figure 2, where the middle root has positive slope $\mathrm{d}R/\mathrm{d}\phi > 0$.

Substituting the homogeneous roots from equation (3.5) into equation (3.2) produces three branches of the constitutive curve (labelled as $1, 2$ and 3, respectively, in Fig. 3). Notice that below a certain shear rate, $\dot{\gamma} = 4$, only the ϕ_1 root is real and the reaction curve is single-valued. This is marked as point P in Figure 3, and has coordinates

$$\{\dot{\gamma}_P, \sigma_P\} = \{4, 2(c+1)\} \,. \tag{3.6}$$

Physically, this means that only species A exists at low (uniform) shear rates. From equation (3.2), we can see that this one-phase system ($\phi_A = 1$) is Newtonian, and the corresponding flow curve has a slope of unity. The slope of the stable flow-induced branch 3 depends on the value of the parameter c. For $c < 1$, a transition from branch 1 to branch 3 is shear thinning, while for $c > 1$ such a transition is shear thickening. The locus of flow-induced roots (ϕ_2, ϕ_3) exhibits a minimum in the shear stress as a function of shear rate, which is denoted as point Q in Figure 3:

$$\{\dot{\gamma}_Q, \sigma_Q\} = \left\{ \frac{(1+\sqrt{c})^2}{\sqrt{c}}, (1+\sqrt{c})^2 \right\} . \tag{3.7}$$

For a given value of the local stress, the homogeneous steady states are given by

$$\phi_1 = 0 \,, \tag{3.8a}$$

$$\phi_{2'} = \frac{(\sigma - c + 1) - \sqrt{(\sigma - c + 1)^2 - 4\sigma}}{2\sigma} \,, \tag{3.8b}$$

$$\phi_{3'} = \frac{(\sigma - c + 1) + \sqrt{(\sigma - c + 1)^2 - 4\sigma}}{2\sigma} \,. \tag{3.8c}$$

Note that these roots are found by recasting equation (3.4) in terms of the stress, by using equation (3.2). This procedure is not equivalent to substituting equation (3.2) into equation (3.5). This is because while the *locus* of homogeneous states is the same under fixed local stress or shear rate, the *stability* of these steady states is not; *i.e.* the portion of the constitutive curve between P and Q is unstable under fixed local stress, but stable under fixed local shear rate. In Figure 3, point Q marks the stress above which the constitutive curve is multivalued for controlled stress, while P marks the strain rate above which the constitutive curve is multivalued for controlled shear rate.

In an experiment, however, only the *average* stress and shear rate can be controlled. If the average shear rate is held fixed at Γ, for example, the system can choose between various options (illustrated in Fig. 3a):

i) A homogeneous low stress state, ϕ_1.
ii) A homogeneous high stress state, $\phi_{3'}$.
iii) A mixture of states i) and ii), where the interfaces between phases lies in the vorticity direction (vorticity banding). Note that i) and ii) cannot coexist with each other in the y-direction, since the stress must be homogeneous in the gradient direction.
iv) A mixture of high shear rate phase, $\phi_{3'}$ and a low shear rate phase, ϕ_1. Here the system attains an intermediate stress, σ^*, and the relative proportions of the two phases are set such that the average shear rate is maintained at Γ. Since the bands have the same stress, but different shear rates, this scenario corresponds to gradient banding.

While it appears from Figure 3 that there is a multiplicity of stresses σ^* at which the system can gradient-band, in fact the system selects a particular stress (see next section).

If, instead, the average stress is fixed at Σ (illustrated in Figure 3b), the system can choose a high or low shear

rate homogeneous phase, or it can gradient-band between these. Alternatively, it can band in the vorticity direction between high and low stress states, by adopting a shear rate γ^*. There is also a selected shear rate for vorticity banding. *The essential question is: which of the many possible states available to it does the system actually choose and why?*

4 Calculating the banding stress and shear rate

The inclusion of gradient terms in equation (2.3) causes stress selection for gradient banding, and shear rate selection for vorticity banding [17]. The selected stress and shear rate are determined by mathematically connecting two different homogeneous stable states to form an inhomogeneous profile. To find the banding shear rate $\dot{\gamma}^*$ at which vorticity banding can occur, equation (2.3) is integrated across the domain at steady state. A banding solution (homogeneous phases separated by interfaces) is, by definition, one that has no gradients in ϕ at the boundaries. We obtain the following condition:

$$\int_{\phi_1(\dot{\gamma}^*)}^{\phi_3(\dot{\gamma}^*)} \mathrm{d}\phi\, R[\phi, \dot{\gamma}^*] = 0\,, \tag{4.1}$$

where ϕ_1 and ϕ_3 are given by equations (3.5). This condition applies for any analytic $R[\phi, \dot{\gamma}]$. Other gradient terms could either lead to a different integral condition, or to no simple integral condition at all. For example, the gradient term $g(\phi)\nabla^2\phi$ leads to the condition $\int_{\phi_1}^{\phi_3} \mathrm{d}\phi\, R[\phi, \dot{\gamma}]/g(\phi) = 0$, while the term $(\nabla\phi)^2$ is not integrable. Note that, by symmetry, only even powers of gradients and a convective term such as $\mathbf{v}\cdot\nabla\phi$ (which drops out anyway) are allowed in planar shear flow.

Defining a new function, $F[\phi, \dot{\gamma}] = \int_0^{\phi} \mathrm{d}\,\phi' R[\phi', \dot{\gamma}]$, we can rewrite equation (4.1) as

$$F[\phi_1(\dot{\gamma}^*), \dot{\gamma}^*] = F[\phi_3(\dot{\gamma}^*), \dot{\gamma}^*]\,, \tag{4.2}$$

which is analogous to the common tangent construction from equilibrium thermodynamics. We note that the interpretation of F as the free energy in an equilibrium phase transition is purely formal and not physical, as this is a dynamic system. Using equation (3.5) in equation (4.2) gives

$$\dot{\gamma}^* = 4.5\,. \tag{4.3}$$

To calculate the banding stress σ^* at which gradient-banding can occur, equation (4.1) must be recast in terms of the shear stress using the stress constitutive relation, equation (3.2) to obtain a relation $\dot{\gamma}(\sigma, \phi)$. The banding stress in our minimal model is only a function of c and is given by the solution of the following equation:

$$F[\phi_{1'}(\sigma^*), \sigma^*] = F[\phi_{3'}(\sigma^*), \sigma^*]\,, \tag{4.4}$$

Table 1. Banding stress σ^*, points of instability P and Q, and coexistence conditions for different values of c. In all cases $\dot{\gamma}_P = 4$ and $\dot{\gamma}^* = 4.5$, while the stress and shear rate on branch ϕ_1 are related by $\sigma_1 = \dot{\gamma}_1$.

c	σ^*	$\phi_3(\sigma^*)$	$\dot{\gamma}(\phi_3^*)$	σ_P	$\dot{\gamma}_Q$	σ_Q
0.3	2.815	0.810	6.504	2.6	4.374	2.395
0.6	3.606	0.732	5.100	3.2	4.066	3.149
1.2	4.910	0.642	4.352	2.4	4.008	4.391
2.7	7.625	0.529	4.014	5.4	4.252	6.986

where $F[\phi, \sigma^*] = \int_0^{\phi} \mathrm{d}\,\phi' R[\phi', \dot{\gamma}(\sigma, \phi')]$ yields

$$F[\phi(\sigma^*), \sigma^*] = \frac{\sigma^*}{(c-1)^4}\left[-\tfrac{1}{3}\tilde{\phi}^3 + \tfrac{1}{2}(c+2)\tilde{\phi}^2 + \tfrac{3}{2}c - (2c+1)\tilde{\phi} + \tfrac{1}{3} + c\ln\tilde{\phi}\right] - \tfrac{1}{2}\phi^2(\sigma^*)\,, \tag{4.5}$$

$$\tilde{\phi} = \phi(\sigma^*)(c-1) + 1, \tag{4.6}$$

and $\phi_{1'}$ and $\phi_{3'}$ are given by equations (3.8). The selected stress σ^* and shear rate $\dot{\gamma}^*$ are shown in Figure 3 for $c = 0.3,\ 2.7$, and given in Table 1.

5 Dynamical selection of steady states

In the preceding sections we have seen that certain homogeneous and banded states are available to the system, based on a *steady-state* analysis and linear-stability considerations. To determine which of these states is selected in practice, equation (2.3) must be evolved in time; to make contact with experiments we can only impose constraints of fixed average shear rate or stress. In this work only one-dimensional calculations are performed, so that the equation of motion is solved either in the y (gradient) or z (vorticity) directions. If there are composition modulations in the y-direction, these can only cause modulations in the shear rate (gradient banding), since the shear stress must be uniform in y. If the average stress is controlled, there is only one "interesting" stress σ^* at which the system can become inhomogeneous in the y-direction. Due to the numerical difficulty of fixing a precise stress in the system, we do not consider this case. By comparison, if the average shear rate is controlled, there is a wide range of shear rates for which we can investigate whether the system remains homogeneous or gradient-bands. Similarly, when composition modulations in z are allowed, we can only look for vorticity banding under controlled stress within this calculation. Gradient banding can occur only if the shear rate is set exactly at $\dot{\gamma}^*$, which we do not study here.

5.1 Controlled average shear rate

We first consider the system under shear rate control, and only allow for spatial variations in y. Integrating the stress relation, equation (3.2), across the domain (where

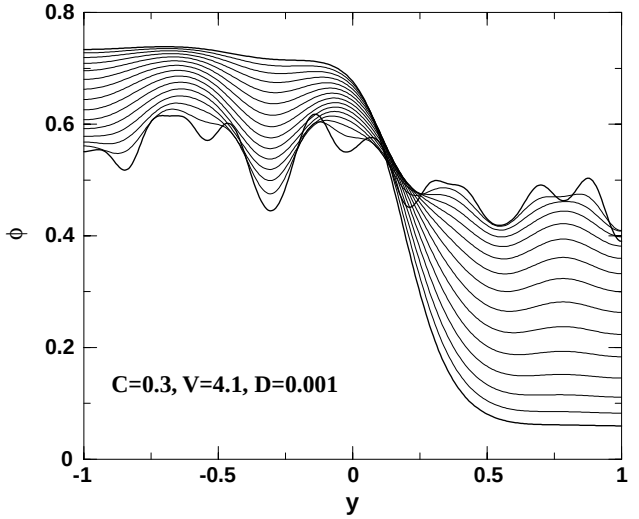

Fig. 4. Time evolution of equation (5.1), for random initial conditions, $c = 0.3, D = 0.001$ and an imposed shear rate $V = 4.1$.

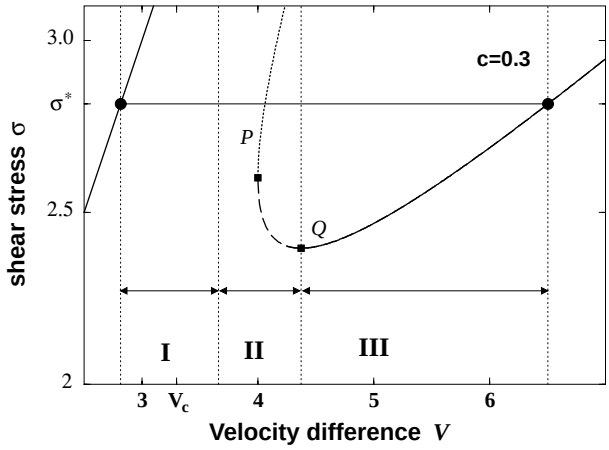

Fig. 5. Basins of attraction for different states, for $c = 0.3$ and imposed mean shear rates $V \equiv \bar{\dot{\gamma}}$. In I the system usually attains the homogeneous flow branch $\phi = \phi_1 = 0$. In II the system usually bands at stress σ^*, and in III the system usually attains the homogeneous state $\phi = \phi_3$. *For $V < V_c \simeq 3.3$ the system always attains the branch $\phi = \phi_1 = 0$.* The behavior is smooth as V is increased through these regimes (see data in Tab. 2).

the shear stress is independent of y) gives the local shear rate as a function of V, the velocity difference across the system. Then equation (2.3) becomes

$$\frac{\partial \phi}{\partial t} = \frac{V}{\int \mathrm{d}y \left\{1/\left[\phi\,(c-1)+1\right]\right\}} \frac{\phi^2(1-\phi)}{\phi(c-1)+1} - \phi + D\frac{\partial^2 \phi}{\partial y^2}\,. \tag{5.1}$$

This is an integro-differential equation, instead of the differential equation that yielded the analysis of Section 3. Notice, however, that the same homogeneous steady states are obtained. Equation (5.1) is solved using random initial conditions with ϕ uniformly chosen within the range $[0-1]$, and no flux boundary conditions, keeping V at a fixed value. The domain size is normalized to unity, so that V is synonymous with the average shear rate.

To solve equations (5.1), we use a fully implicit finite-difference scheme, using a central difference approximation for first and second spatial derivatives, and a forward difference approximation for the time derivative. Nonlinear terms are linearized in time as follows:

$$W[\phi(x,t+\Delta t)] = W[\phi(t)] + [\phi(t+\Delta t) - \phi(t)]\frac{\partial\, W[\phi,t]}{\partial \phi}. \tag{5.2}$$

The integral in equation (5.1) is evaluated explictly, *i.e.* at the previous time step. In general, 300 spatial mesh points are used with a time step of 1/10000 [21].

For some initial conditions the resulting steady states are homogeneous, while for others they are banded. (Fig. 4 shows the evolution of the system to a banded state, for one such set of initial conditions.) This implies that there is a *basin of attraction* for attaining a banded state. Our results can be categorized according to the shape of the constitutive curve and the magnitude of the diffusion coefficient, and whether the system is shear thinning or thickening. We find that decreasing the diffusion coefficient increases the basin of attraction of the banded state and destabilizes the homogeneous state. That is, the system is more likely to band for narrow interfaces. Intuitively, this makes sense since the banded state represents a mathematical connection between two homogeneous states: the wider the interface, the more difficult it is for gradients to be nonzero near the boundaries of the system. For $c < 1$, the system crosses over from a homogeneous state on branch 1 to a banded state much before $V = \dot{\gamma}_P$. Notice that banding is first allowed, in principle, when the imposed shear rate is larger than that of the low shear rate band at the selected stress σ^*. The "critical" mean shear rate V_c, where the system actually first starts to band, is generally somewhat higher than this: hence, V_c is the low shear rate limit of the stress plateau that would be measured experimentally. Below V_c the system *always* chooses the homogeneous state, and the exact value of V_c depends on the diffusion coefficient D, with a smaller V_c for smaller values of D. Increasing the diffusion coefficient widens the interface, affecting where the interface first "touches" the wall [13] and the ability of a banded system to satisfy the boundary conditions, as discussed above.

For a window of applied mean shear rates V roughly in the region $\dot{\gamma}_P < V < \dot{\gamma}_Q$, the system is more inclined to band than to remain homogeneous (see Fig. 5). The crossover to a situation where homogeneous states are preferred to banded states occurs for $V \geq \dot{\gamma}_Q$, with the crossover at a higher V for smaller values of the diffusion coefficient. The chosen homogeneous states always lie on branch 3 of the constitutive curve. This shows that the system has made a transition under flow, so that for $c < 1$ a shear-thinning transition is seen, as discussed in section 3. These findings are illustrated in Table 2, for 49 runs with different initial conditions with $c = 0.3$. The

Table 2. Summary of results for $c = 0.3$, for 49 runs with random initial conditions and controlled mean shear rate V. In this case, $\dot{\gamma}_P$ corresponds to $V = 4.0$, and $\dot{\gamma}_Q$ corresponds to $V = 4.374$. Banding is first allowed at $V = 2.815$.

V	D	ϕ_1	Result banded	ϕ_3
3.3	0.01	49	0	0
	0.005	49	0	0
	0.001	48	1	0
3.6	0.01	45	5	0
	0.005	34	15	0
	0.001	6	43	0
3.8	0.01	15	34	0
	0.005	8	41	0
	0.001	0	49	0
3.9	0.01	0	49	0
	0.005	0	49	0
	0.001	0	49	0
4.0	0.01	0	49	0
	0.005	0	49	0
	0.001	0	49	0
4.05	0.01	0	49	0
	0.005	0	49	0
	0.001	0	49	0
4.1	0.01	0	49	0
	0.005	0	49	0
	0.001	0	49	0
4.25	0.01	0	39	10
	0.005	0	47	2
	0.001	0	49	0
4.37	0.01	0	10	39
	0.005	0	33	16
	0.001	0	49	0
4.4	0.01	0	10	39
	0.005	0	21	28
	0.001	0	49	0
4.55	0.01	0	2	47
	0.005	0	8	41
	0.001	0	13	36
4.6	0.01	0	1	48
	0.005	0	7	42
	0.001	0	20	29
4.7	0.01	0	0	49
	0.005	0	4	45
	0.001	0	19	30

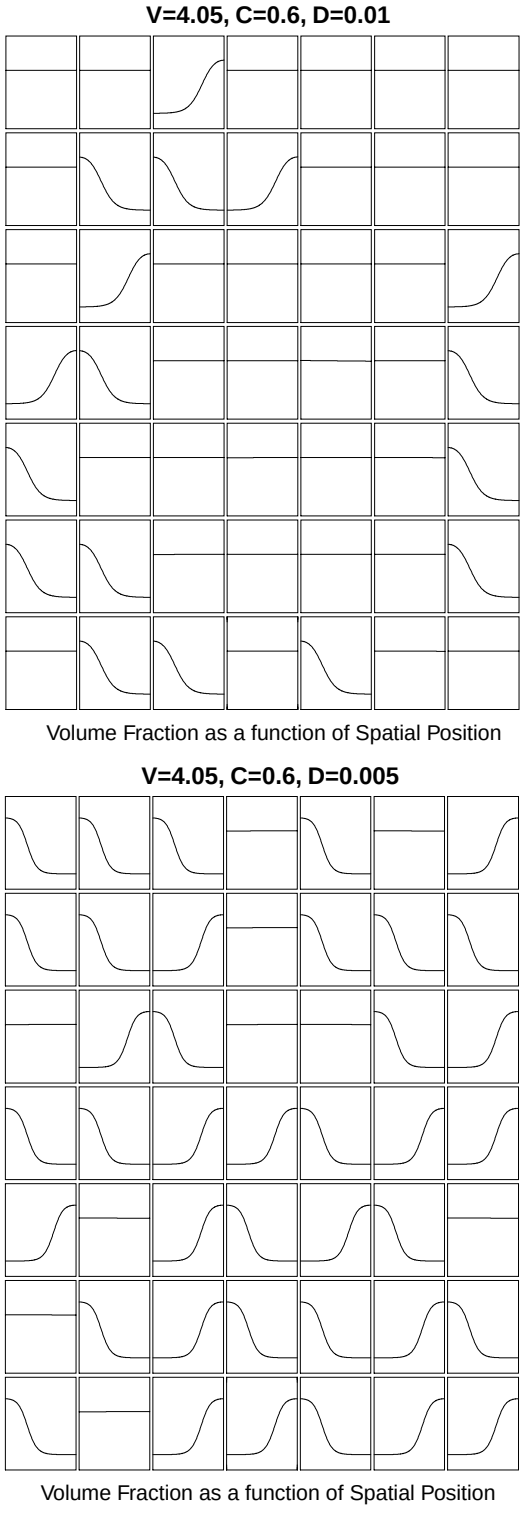

Fig. 6. Steady-state composition profiles for 49 runs with random initial conditions, for $c = 0.6$ and imposed shear rate $V = 4.05$. Here, $\dot{\gamma}_P$ corresponds to $V = 4.0$, and $\dot{\gamma}_Q = 4.066$.

"critical" shear rate in this case is $V_c \simeq 3.3$. Figures 6 and 7 show a similar behavior for $c = 0.6$.

Gradient banding is never observed in our numerical experiments when $c > 1$. Here, the chosen final steady state, above the critical shear rate, is always the stable high stress homogeneous state on branch 3, which makes this a shear-thickening transition.

The preceding results are for the case where the shear rate is held at a steady value, and might apply to a system where the mean shear rate is applied to an initially noisy system. However, most experiments are conducted by starting up the system from zero shear rate, and then discontinuously ramping the shear rate to higher values. We have tried to mimic this scenario, by bringing the system to steady state for $V < \dot{\gamma}_P$, and then suddenly increasing the value of V to beyond $\dot{\gamma}_P$. In order to dislodge

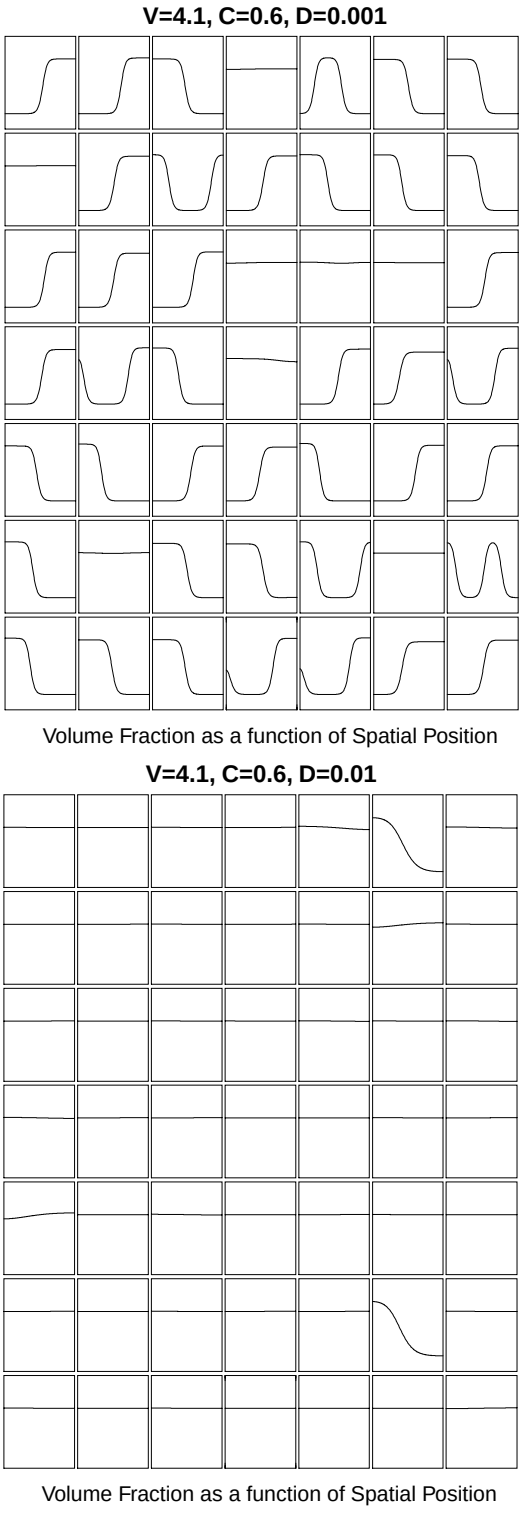

Fig. 7. Steady-state composition profiles for 49 runs with random initial conditions, for $c = 0.6$ and imposed shear rate $V = 4.1$

Table 3. Summary of results for $c = 2.7$, for 49 runs with random initial conditions and controlled stress Σ. In this case, $\sigma_P = 5.4$ and $\sigma_Q = 6.896$.

Σ	D	ϕ_1	Result banded	ϕ_3
5.0	0.01	49	0	0
	0.005	49	0	0
	0.001	49	0	0
5.4	0.01	49	0	0
	0.005	49	0	0
	0.001	49	0	0
6.0	0.01	49	0	0
	0.005	48	1	0
	0.001	36	13	0
7.1	0.01	28	21	0
	0.005	0	49	0
	0.001	0	49	0
7.2	0.01	0	4	45
	0.005	0	40	9
	0.001	0	49	0
7.3	0.01	0	0	49
	0.005	0	9	40
	0.001	0	43	6
7.4	0.01	0	0	49
	0.005	0	2	47
	0.001	0	23	26
7.5	0.01	0	0	49
	0.005	0	0	49
	0.001	0	13	36
8.5	0.01	0	0	49
	0.005	0	0	49
	0.001	0	0	49

the system from branch 1 to the banded state, however, we need to add noise of amplitude order unity. Such a large amount of noise essentially obliterates any memory of the initial steady state, suggesting that a nucleation event is required for an experimental system to band from start-up, as was found previously in reference [13].

In general, the banded state consists of two bands, corresponding to branches 1 and 3 on the constitutive curve. For some initial conditions, multiple bands are found. The runs denoted as "banded" in Table 2 do not differentiate between these banding configurations. We do not attach much significance to multiple banding, because it is known that several interfaces are allowed for planar flow, and the number of allowed interfaces in such one-dimensional systems is known to increase as the diffusion coefficient decreases [22]. Britton and Callaghan have reported multiple gradient bands for wormlike micelles in Couette flow [7]. However, it has been shown [13] that simple constitutive relations (like the one derived here) do not permit multiple interfaces in Couette flow. This implies that the current model cannot describe these experimental observations.

5.2 Controlled average stress

Next we fix the average shear stress and solve the model in the z-direction, hence allowing for vorticity banding at different stresses. Following a procedure analogous to that of the previous section, the observation that the shear rate

is uniform in z allows us to convert equation (2.3) into the following integro-differential equation:

$$\frac{\partial \phi}{\partial t} = \frac{\Sigma\, \phi^2(1-\phi)}{\int \mathrm{d}z[\phi(c-1)+1]} - \phi + D\frac{\partial^2 \phi}{\partial z^2}, \qquad (5.3)$$

where Σ is the imposed average shear stress across the domain.

Note that interchanging the stress and shear rate variables in the phenomenological model would "reverse" all the results of Section 5.1. Thus, branch 3 would be thickening for $c < 1$, and the system would be inclined to vorticity band under stress control, around $\sigma_P < \Sigma < \sigma_Q$. Similarly, the system would remain homogeneous for $c < 1$. This reasoning implies that the shape of the flow curve sets the attractors for the system. If this is true, then when stress and shear rate are not interchanged, the system should be predisposed to vorticity band for $c > 1$ when the stress is fixed between σ_P and σ_Q, but should remain homogeneous for all stresses when $c < 1$.

This is indeed what we find from numerical solution of equation (5.3). Table 3 shows results for $c = 2.7$ and various values of Σ. Decreasing the diffusion coefficient destabilizes the homogeneous state, as in the controlled shear rate case.

We sometimes observe multiple bands under stress control, as with the fixed shear rate cases. Bonn *et al.* [2] and Chen *et al.* have seen multiple bands in the vorticity direction in Couette flow which is probably due to a combination of the slow coarsening expected in one-dimensional systems [23] and multiple allowed interfaces [22]. The stress is nonuniform and monotonic in the flow gradient direction of a cylindrical Couette device, which implies a single stable interface. The cylindrical geometry does not, however, impose such an inhomogeneity along the vorticity direction.

6 Conclusions

We have shown that a simple phenomenological reaction-diffusion scheme can produce a flow-induced phase transition, as a consequence of a multi-valued reaction term. The model consists of an equation of motion for a nonconserved composition variable, while the stresses induced in the reactants and products are assumed to be fast variables. The character of the model depends on a single parameter c, that controls whether or not the transition is shear thinning or shear thickening. Above a critical shear rate (or shear stress), the system may band or remain homogeneous. The steady states that are selected from random initial conditions depend on the shape of the constitutive curves and the magnitude of the diffusion coefficient:

1. *Imposed shear rates:* For $c < 1$ (shear-thinning transition), the system chooses a low-stress homogeneous state at low shear rates. Above a critical shear rate, gradient banding tends to occur for imposed shear rates around the region of the constitutive curve with negative slope $\mathrm{d}\sigma/\mathrm{d}\dot{\gamma} < 0$ (see Fig. 3a). At shear rates higher than this, the system is predisposed towards the high stress homogeneous state. For $c > 1$ (shear-thickening transition), the system always chooses this homogeneous state above the critical shear rate and gradient banding is never observed.
2. *Imposed stress:* For $c > 1$ (shear-thickening transition), the system chooses a low shear rate homogeneous at low stresses. Above a critical stress, vorticity banding tends to occur for imposed stresses around the region of the constitutive curve with negative slope. For higher stresses, the system is predisposed towards the high shear rate homogeneous state. For $c < 1$, the system always chooses this homogeneous state above the critical stress and vorticity banding is never observed.
3. In the regions of the flow curve where banding is observed, we find that the apparent basin of attraction for banding increases upon decreasing the value of the diffusion coefficient.

While banding is more pronounced in the vicinity of the flow curve with a negative slope (where the system is linearly unstable for controlled stress), it is also observed in regions of the flow curve with positive slope. In particular, the critical shear rate or stress (where banding is first initiated), lies in the latter section of the flow curve. Here, the system is nonlinearly unstable to perturbations. Such behavior has been seen in experiments on shear-thinning wormlike micelles [24], where the onset of banding occurs at a lower stress (and shear rate) if the system is given enough time to explore all fluctuations, as compared to where banding is induced upon rapidly varying the control parameters. Porte *et al.* [25] have discussed various flow curves that can contain both linearly and nonlinearly unstable regions: the equilibrium analog of the former is the spinodal curve, and that of the latter is the metastable region, where an instability must be nucleated.

Our results are significant because they show that a minimal model can exhibit a rich phenomenology, and that the selection rules for phase coexistence are simple. To understand why the system chooses certain states over others in some regions of the flow curve, a nonlinear dynamics analysis of the model must be performed. We believe that our scheme represents a new class of reaction-diffusion equations, because the constraint of fixed average stress or shear rate turns the governing partial differential equations into integro-differential equations, which represents a general class of dynamical equations that, to our knowledge, has not been studied. This system exhibits fascinating and complex nonlinear dynamics that we will discuss in a future publication.

Since the shape of the constitutive curve impacts the choice of banded states, examination of the generality of the reaction terms is warranted. For example, it is known [22,26] that the slopes of the crossings and the steepness of the extrema of the reaction curve can change the interfacial profile and velocity, which can affect the system dynamics.

Our current scheme is missing much physics: a complete model would involve coupled equations of motion for conserved variables (concentration of the various species)

and nonconserved, tensorial variables (structural variables, stress), as well as the Navier-Stokes dynamics for the fluid velocity (momentum). The momentum degrees of freedom are particularly important, and would qualitatively change the nature of the basin of attraction we have found. Regions of the composite flow curve with negative slope (between points P and Q in Fig. 3) would have unstable homogeneous states, so that the homogeneous states in Table 2, for $V = 4.25$ and $V = 4.37$, would not be found. Also, we have assumed that the individual species obey Newtonian stress constitutive relations. Typically, these species are themselves complex fluids, and are either shear thinning or exhibit a yield stress. In future work, by systematic exclusion of certain dynamic variables, we will be able to investigate the individual roles played by the stress, concentration, etc., in order to determine which variables are essential to the problem formulation.

One of us [15] has already considered a theory with stress, momentum and concentration variables in the context of rigid rod suspensions. Separate phase diagrams for shear-induced phase separation in both the vorticity and gradient directions were calculated, but the model was too prohibitively complicated to study which of these orientations would in fact be selected by the system. In this work, we have used a much simpler scheme to demonstrate the neccessary analysis (albeit within a one-dimensional model—see next paragraph) to unambiguously determine whether banding actually occurs in a system, as well as the banding orientation. While Schmitt *et al.* [10] have also presented quite a simple phenomenological model (including both concentration and momentum as dynamical variables), they did not go beyond a linear-stability analysis. They also did not consider the case (as we have here) of a nonconserved variable initiating an instability in the system.

Our calculations have been carried out only for the case of planar flow. It has been shown for the Johnson-Segalman model [13] that the nonuniformity of stress in a curved geometry has significant effects on banding. In addition, we have examined the issue of gradient *vs.* vorticity banding using a one-dimensional model. Realistically, the model should be solved considering both vorticity and gradient directions simultaneously. The band orientation may be influenced by anisotropy in the diffusion coefficient. A convective term of the form $\mathbf{v} \cdot \nabla \phi$ should also be included in the equation of motion. Such a term does not appear in a one-dimensional shear flow, but it can qualitatively affect transients in phase separation in two dimensions. Finally, noise has been incorporated into our model through the initial conditions. While Gaussian noise is present in the equation of motion through the diffusion term, in a driven system there may be other noise terms that should be added.

We stress that our phenomenological theory only aims to describe the general macroscopic physics of flow-induced phase transitions. Details concerning the underlying structural transformations can only be probed by more specific microscopic models.

References

1. P. Boltenhagen, Y.T. Hu, E.F. Matthys, D.J. Pine, Europhys. Lett. **38**, 389 (1997).
2. D. Bonn, J. Meunier, O. Greffier, A. Alkahwaji, H. Kellay, Phys. Rev. E **58**, 2115 (1998).
3. E. Eiser, F. Molino, G. Porte, Rheol. Acta **39**, 201 (2000); Phys. Rev. E **61**, 6759 (2000).
4. L. Noirez, A. Lapp, Phys. Rev. Lett. **78**, 70 (1997).
5. L.B. Chen, C.F. Zukoski, B.J. Ackerson, H.J.M. Hanley, G.C. Straty, J. Barker, C.J. Glinka, Phys. Rev. Lett. **64**, 688 (1992).
6. P.D. Olmsted, Europhys. Lett. **48**, 339 (1999).
7. M.M. Britton, P.T. Callaghan, J. Rheol. **41**, 1365 (1997).
8. L. Ramos, F. Molino, G. Porte, Langmuir **16**, 5846 (2000).
9. J.L. Goveas, D.J. Pine, Europhys. Lett. **48**, 706 (1999).
10. V. Schmitt, C.M. Marques, F. Lequeux, Phys. Rev. E **52**, 4009 (1995).
11. N.A. Spenley, X.F. Yuan, M.E. Cates, J. Phys. II **6**, 551 (1996).
12. X.F. Yuan, Europhys. Lett. **46**, 542 (1999).
13. P.D. Olmsted, O. Radulescu, C.-Y.D. Lu, J. Rheol. **44**, 257 (2000).
14. M.E. Cates, Macromolecules **20**, 2289 (1987); J. Phys. Chem. **94**, 371 (1990).
15. P.D. Olmsted, P.M. Goldbart, Phys. Rev. A **41**, 4578 (1990); **46**, 4966 (1992); P.D. Olmsted, C.-Y.D. Lu, Phys. Rev. E **56**, 55 (1997); **60**, 4397 (1999).
16. A. Ajdari, Phys. Rev. E **58**, 6294 (1998).
17. C.-Y.D. Lu, P.D. Olmsted, R.C. Ball, Phys. Rev. Lett. **84**, 642 (2000).
18. O. Diat, D. Roux, J. Phys. II **3**, 9 (1992).
19. M.E. Cates, M.S. Turner, Europhys. Lett. **11**, 681 (1990).
20. G.H. Fredrickson, L. Leibler, Macromolecules **29**, 2674 (1996).
21. In the numerical solution of the integro-differential equation, we observe a small (on the order of a few tenths of a percent) variation with mesh size of the steady-state selected stress of the banded states.
22. P. Grindrod, *The Theory and Applications of Reaction-Diffusion Equations: Patterns and Waves* second edition (Clarendon Press, Oxford, 1996).
23. N. Alikakos, P.W. Bates, G. Fusco, J. Differ. Equ. **90**, 81 (1991).
24. C. Grand, J. Arrault, M.E. Cates, J. Phys. II **7**, 1071 (1997).
25. G. Porte, J.F. Berret, J. Harden, J. Phys. II **7**, 459 (1997).
26. W. van Saarloos, Phys. Rep. **301**, 9 (1998).